Supplementary information to:

Enhancing micropollutant removal efficiency using sustainable activated charcoal

Taher Selmi[1,2,*], Solène Gentil[2], Vanessa Fierro[1], Alain Celzard[1,3,*]

[1] Université de Lorraine, CNRS IJL, F-88000 Epinal, France

[2] Groupe BORDET, Froidvent, F-21290 Leuglay, France

[3] Institut Universitaire de France (IUF), F-75231 Paris, France

[*] Corresponding authors. E-mails: taher.selmi@univ-lorraine.fr; alain.celzard@univ-lorraine.fr

I. Textural characterization

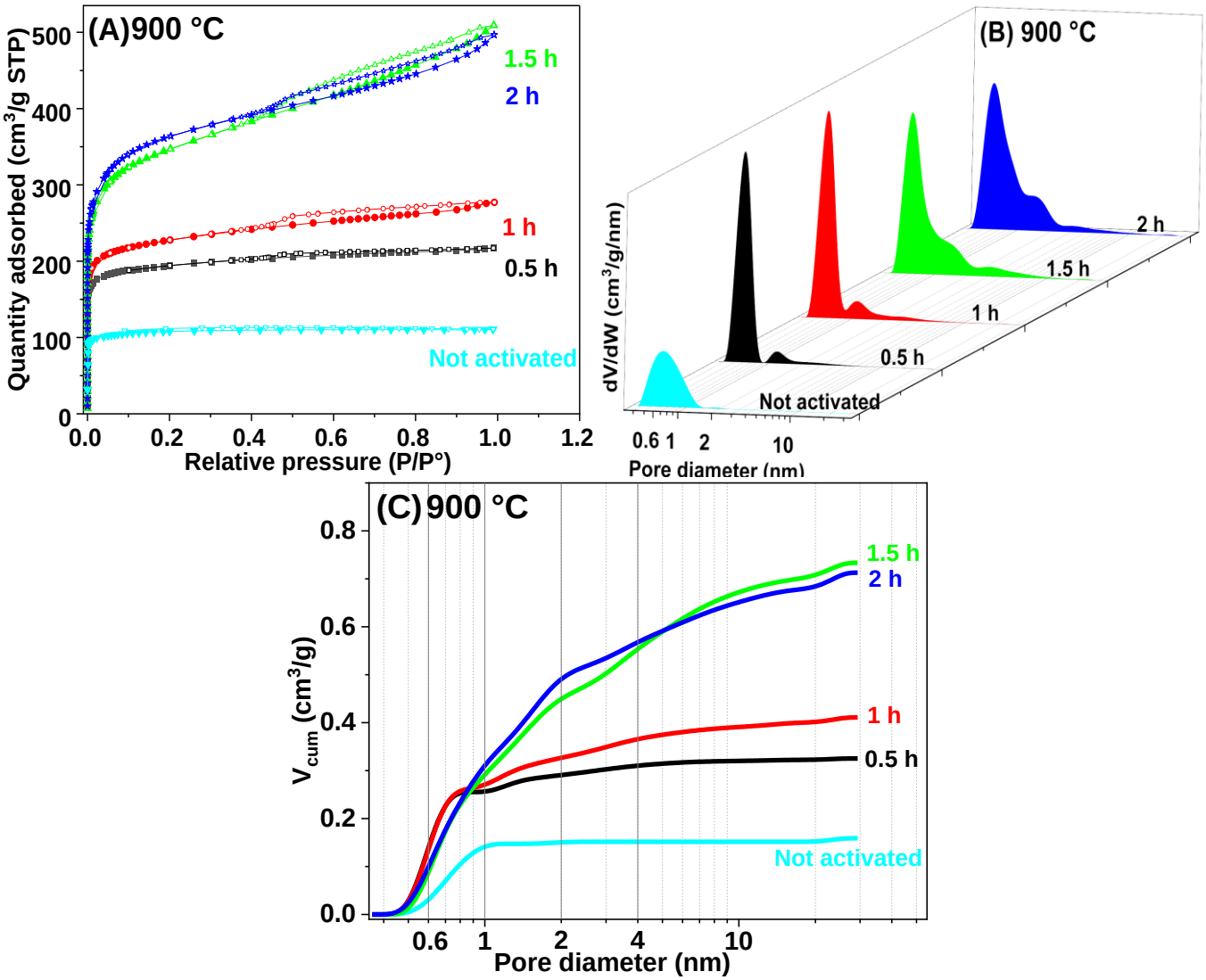

Figure SI 1: (A) N_2 adsorption-desorption isotherms; (B) pore size distributions (PSD); and (C) cumulative pore volumes of charcoal activated at 900 °C and different activation times.

Table SI 1: Textural properties of ACs and burn-off (BO) as a function of activation time and temperature.

Activation temperature	Parameters	**0 h**	**0.5 h**	**1 h**	**1.5 h**	**2 h**	**2.5 h**
850 °C	BO (%)	0	19.50	38.24	49.00	56.14	69.70
	A_{BET} (m^2/g)	400	600	855	1045	1110	1380
	V_{mes} (%)	6.5	9	31	34	33.5	41
	V_{mic} (cm^3/g)	0.17	0.23	0.33	0.40	0.42	0.51
	V_{tot} (cm^3/g)	0.18	0.25	0.48	0.60	0.63	0.87
900 °C	BO (%)	0	29.50	43.00	57.00	68.23	-
	A_{BET} (m^2/g)	400	760	880	1290	1355	-
	V_{mes} (%)	6.5	12	23	39	33	-
	V_{mic} (cm^3/g)	0.17	0.30	0.33	0.48	0.50	-
	V_{tot} (cm^3/g)	0.18	0.34	0.43	0.78	0.75	-

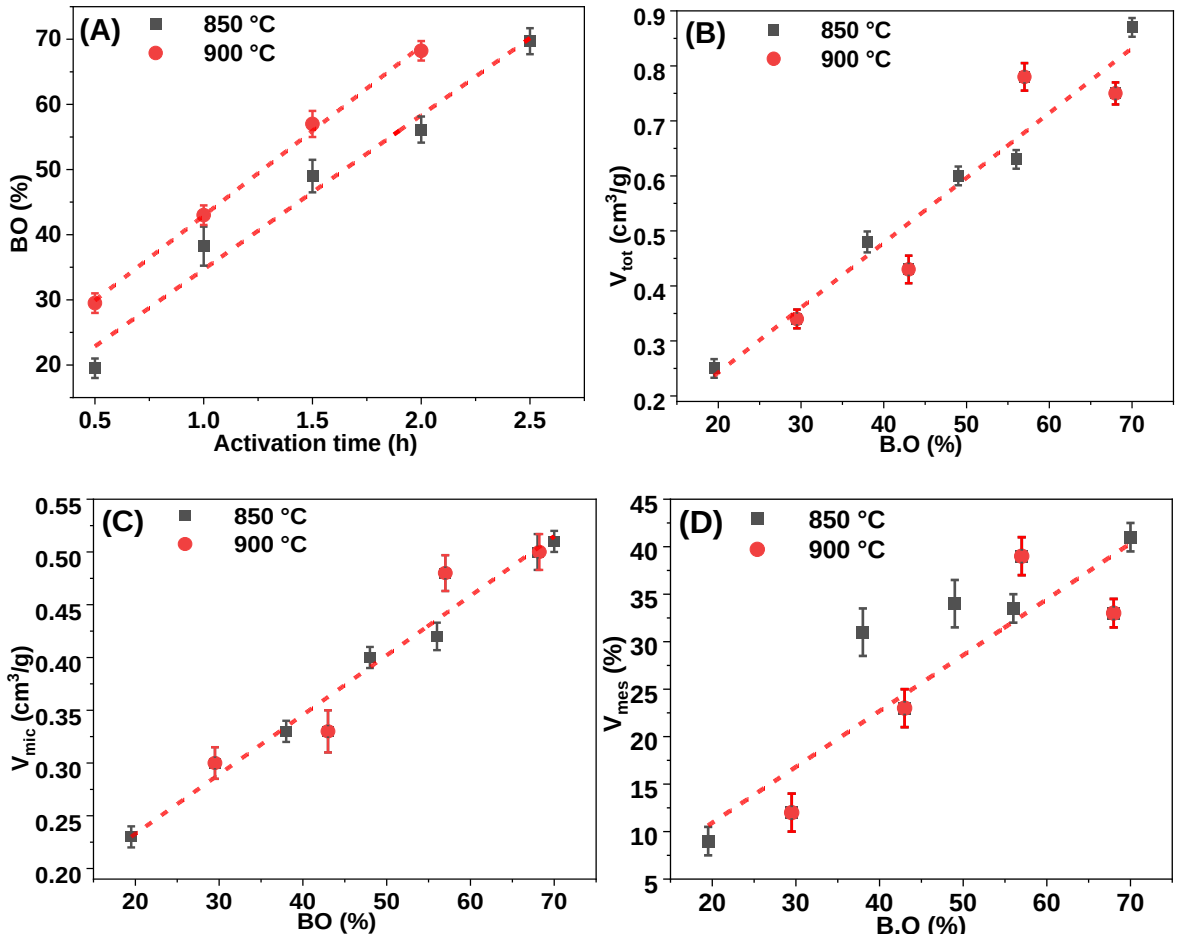

Figure SI 2: Effect of activation time and temperature on the textural properties of ACs derived from Groupe Bordet's charcoal.

II. Chemical characterization

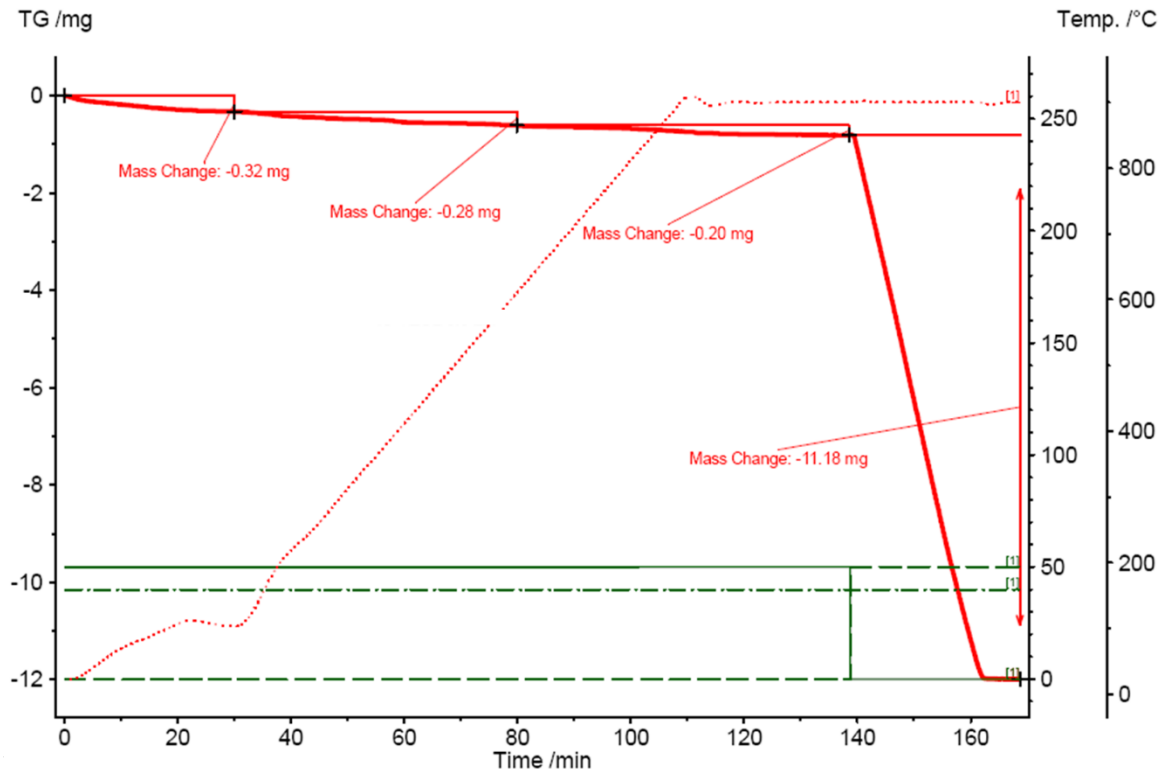

Figure SI 3: Thermogravimetric analysis of sample AC850°C-2h.

Table SI 2: pH_{PZC} and pKa of the main surface functional groups of AC samples and their corresponding amounts (in parenthesis, mmol/g) determined by potentiometric titration.

Samples	**Non-activated charcoal**	**AC850°C-2h**	**Brita AC**	**F300**
***pK*$_a$ 3–5**	-	4.08 (0.07)	4.34 (0.03)	-
***pK*$_a$ 5–7**	-	6.02 (0.05)	6.58 (0.04)	5.38 (0.08)
***pK*$_a$ 7–8**	-	7.59 (0.04)	-	-
***pK*$_a$ 8–10**	-	-	8.03 (0.04)	-
***pK*$_a$ 10–12**	10.62 (1.14)	10.09 (0.69)	10.13 (0.51)	10.63 (0.53)
Total acid (mmol/g)	0.00	0.15	0.10	0.08
Total basic (mmol/g)	1.14	0.69	0.51	0.53
***pH*$_{PZC}$**	-	9.3	-	9.0

III. Adsorption kinetics studies

Table SI 3: Adsorbent performance data for different micropollutants, and parameters of the various adsorption kinetic models applied.

	ATZ	DEA	MET ESA	PARA	CBZ	CIP	17 BE	PFOS	PFOA	PFHxA
$Q_{e,\,exp}$	9.85	23.69	31.93	92.83	75.93	66.57	38.13	23.94	4.99	74.62
PFO										
$q_{e,1}$	9.89	23.24	30.39	87.44	70.65	68.83	39.19	24.01	4.73	66.56
k_1	0.057	0.008	0.005	0.040	0.006	0.002	0.003	0.018	0.021	0.023
R^2	0.9995	0.9985	0.9044	0.9748	0.9683	0.9738	0.9974	0.9998	0.9926	0.9451
χ^2	0.005	0.124	9.720	25.167	22.549	9.579	0.502	0.017	0.024	35.335
h_1	0.56	0.19	0.15	3.50	0.42	0.14	0.12	0.43	0.10	1.53
PSO										
$q_{e,2}$	10.56	26.89	32.71	94.94	80.69	89.61	49.59	25.56	5.16	72.82
k_2	0.010	3.426E-4	2.473E-4	5.976E-04	1.001E-04	2.022E-05	4.864E-05	0.001	0.006	4.34E-04
R^2	0.9772	0.9909	0.9556	0.9955	0.9965	0.9840	0.9922	0.9862	0.9980	0.9844
χ^2	0.232	0.741	4.512	4.478	2.514	5.860	1.495	1.468	0.007	10.036
h_2	1.12	0.25	0.26	5.39	0.65	0.16	0.12	0.65	0.16	2.30
BSf (n,α)										
$q_{e,BSf}$	9.86	23.69	70.86	92.16	82.46	106.05	38.13	23.94	5.09	74.81
n	1.06	1.06	3.00	0.41	1.51	0.72	0.75	1.18	3.00	0.56
τ_C	17.42	132.12	1081.68	70.61	172.35	1811.75	397.41	51.59	27.29	127.74
$\tau_{1/2}$	12.86	91.47	2563.07	9.42	136.04	870.21	258.42	40.99	34.23	26.82
α	1.14	0.94	0.47	0.28	0.78	0.63	1.05	1.32	1.79	0.33
R^2	0.9999	0.9995	0.9986	0.9769	0.9999	0.9996	0.9986	1.0000	0.9998	0.9978
χ^2	0.001	0.041	0.138	23.113	0.057	0.144	0.271	0.0000	7.72E-04	1.44

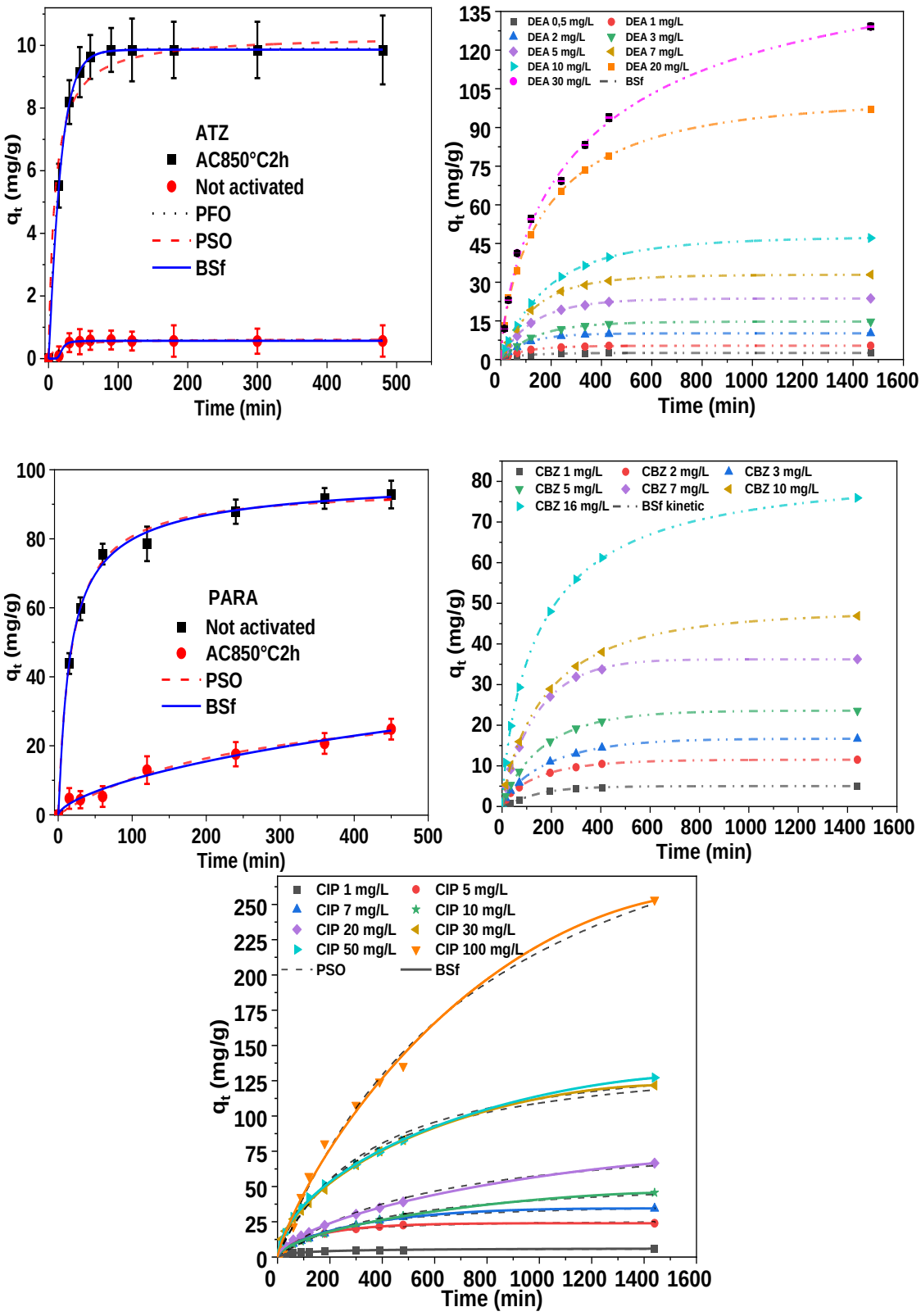

Figure SI 4: Kinetics studies of ATZ and PARA adsorption on AC850°C2h and non-activated charcoal, and DEA CBZ and CIP adsorption on AC850°C2h at different initial concentrations.

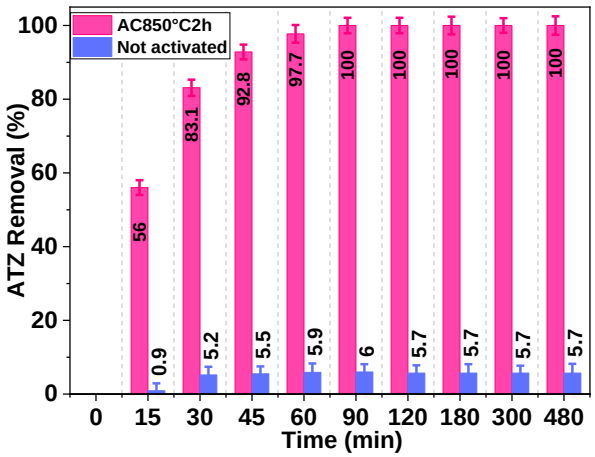
AC850°C2h
Not activated
ATZ Removal (%)
Time (min)
0 15 30 45 60 90 120 180 300 480
56 83.1 92.8 97.7 100 100 100 100 100
0.9 5.2 5.5 5.9 6 5.7 5.7 5.7 5.7

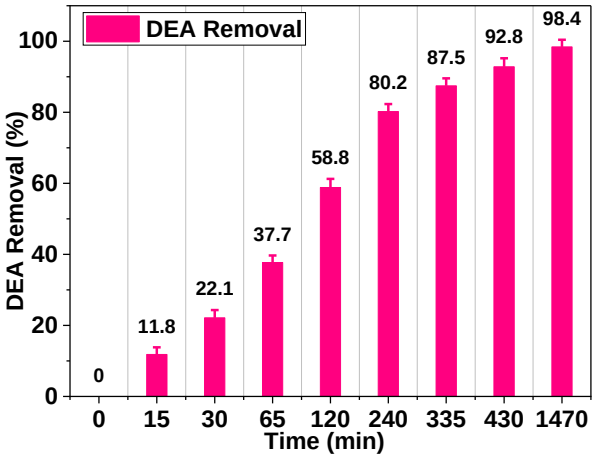
DEA Removal
DEA Removal (%)
Time (min)
0 15 30 65 120 240 335 430 1470
0 11.8 22.1 37.7 58.8 80.2 87.5 92.8 98.4

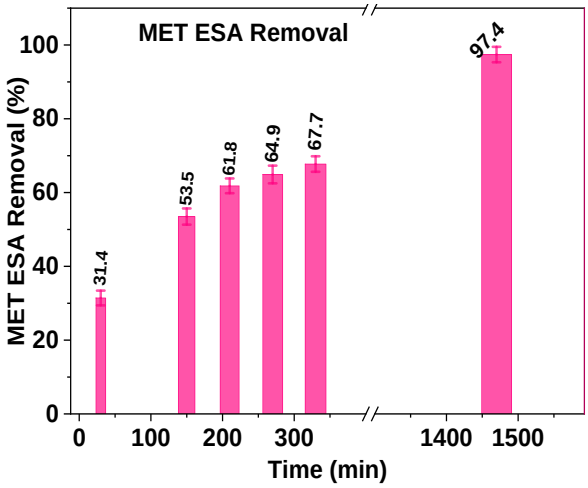
MET ESA Removal
MET ESA Removal (%)
Time (min)
0 100 200 300 1400 1500
31.4 53.5 61.8 64.9 67.7 97.4

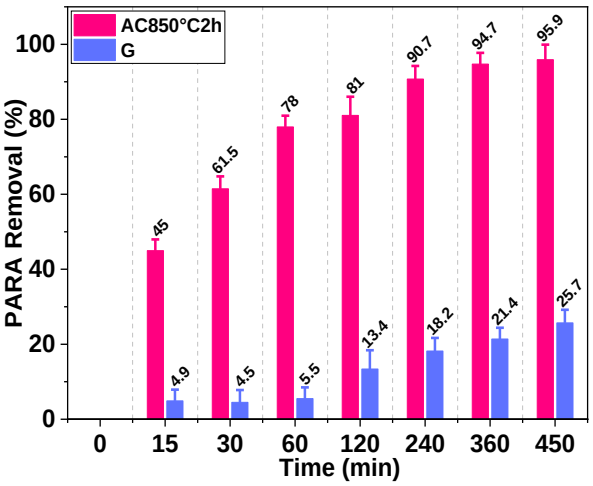
AC850°C2h
G
PARA Removal (%)
Time (min)
0 15 30 60 120 240 360 450
45 61.5 78 81 90.7 94.7 95.9
4.9 4.5 5.5 13.4 18.2 21.4 25.7

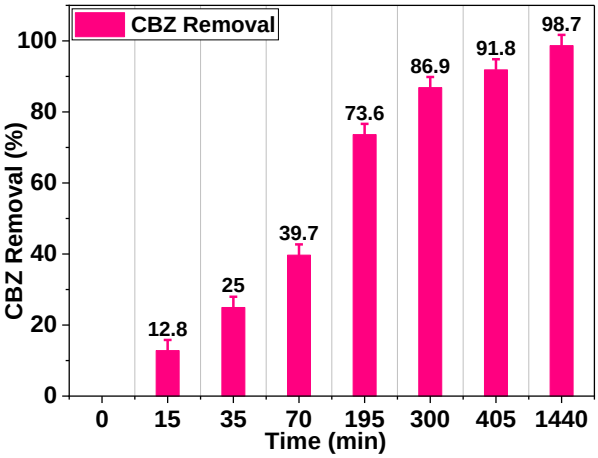
CBZ Removal
CBZ Removal (%)
Time (min)
0 15 35 70 195 300 405 1440
12.8 25 39.7 73.6 86.9 91.8 98.7

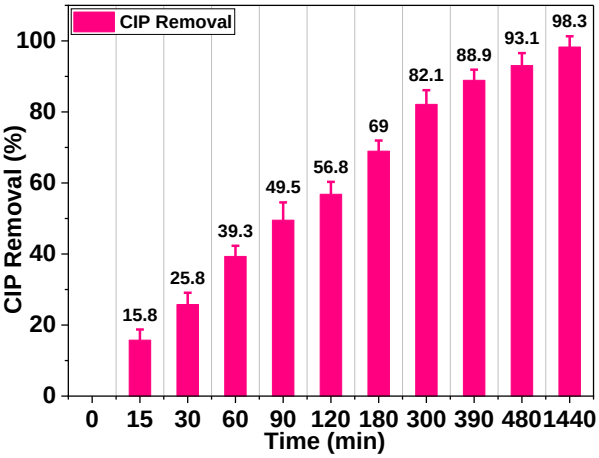
CIP Removal
CIP Removal (%)
Time (min)
0 15 30 60 90 120 180 300 390 480 1440
15.8 25.8 39.3 49.5 56.8 69 82.1 88.9 93.1 98.3

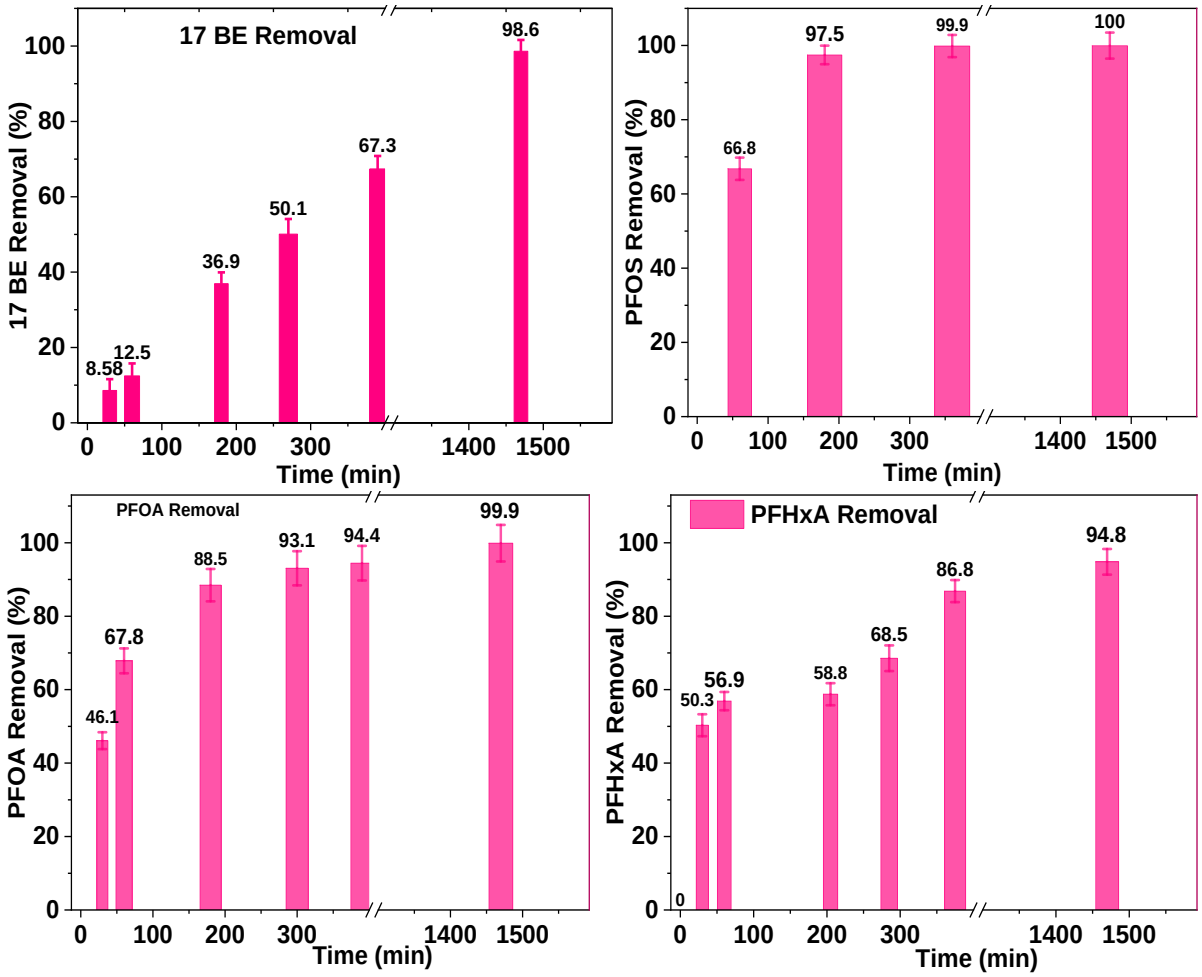

Figure SI 5: Evolution of pesticides (ATZ, DEA and MET ESA), pharmaceuticals (PARA, CBZ, 17 BE and CIP) and PFAS (PFOS, PFOA and PFHxA) removal by AC850°C2h as function of time.

IV. Adsorption isotherm studies

Table SI 4: Parameters of the different isotherm models applied to the equilibrium adsorption of different micropollutants.

	ATZ	DEA	MET ESA	PARA	CBZ	CIP	17 BE	PFOS	PFOA	PFHxA
$q_{e,max,\ exp}$	95.95	129.14	165.23	395.97	75.93	253.29	57.07	669.47	1977.3	3134.71
Freundlich										
K_F	303.45	75.10	39.21	113.38	103.94	39.15	77.81	196.24	106.25	1.83
n_F	1.14	2.55	2.40	4.52	1.53	2.35	3.44	4.44	1.59	0.84
R^2	0.8296	0.9456	0.9306	0.9251	0.8989	0.8848	0.7673	0.8467	0.8233	0.9828
χ^2	195.33	106.68	261.82	1754.64	60.87	754.47	98.29	11.71E3	13.79E4	21.44E3
Langmuir										
$q_{e,max,L}$	370.73	148.35	233.60	411.48	131.20	282.15	59.86	674.32	3549.80	1.77E8
K_L	1.28	1.56	0.08	0.07	2.08	0.06	59.01	0.10	0.01	3.33E-8
R^2	0.8482	0.9696	0.9142	0.9522	0.8892	0.7967	0.9039	0.8665	0.8662	0.9723
χ^2	174.01	59.60	323.62	1121.18	66.72	1331.73	40.59	10.20E3	10.44E4	3.45E4
GBS										
$q_{e,max,GBS}$	92.59	206.12	187.50	398.75	176.92	474.99	56.82	678.05	2090.63	3209.96
a	2.28	0.50	0.74	0.61	0.56	0.47	0.89	0.45	2.64	2.48
b	0.12	4.21	12.58	23.10	2.52	168.60	0.02	18.66	40.23	301.59
c	9.84E-14	5.73E-8	3.22E-7	5.24E-8	5.69E-7	8.09E-8	9.99E-8	7.04E-7	1.77E-7	1.26E-6
$C_{e1/2}$	0.10	2.02	7.67	12.67	1.31	77.3	0.01	8.26	35.02	260.16
R^2	0.9291	0.9435	0.8587	0.9505	0.7321	0.8868	0.9197	0.7836	0.9586	0.9669
χ^2	81.29	110.90	532.84	1159.12	161.25	741.65	33.92	16.53E3	32.32E3	41.25E3
MLM2E										
n_1	0.00	1.08	2.51	0.15	14.00	0.36	1.17	4.78	0.51	0.42
n_2	3.47	3.64	4.18	3.52	1.50	12.93	0.00	5.30	23.37	6.96
D_1	365.03	45.52	54.86	4955.09	1.90	874.30	49.63	17.56	608.18	1.20E6
D_2	27.16	22.13	7.41	54.80	1684.90	5.16E7	0.00	101.52	73.94	334.64
C_1	138.68	0.09	8.65	27.75E4	0.08	86.17	0.02	0.001	0.81	2.34E9
C_2	0.10	0.88	0.01	19.54	8.26	207.41	0.21	10.95	32.84	263.93
$q_{e,max,\ 1}$	0	49.16	137.7	743.26	26.6	314.75	58.07	83.94	310.17	5.04E5
$q_{e,max,\ 2}$	94.25	80.55	30.97	192.9	2527.35	6.67E8	0	538.06	1727.98	0.02E5
$q_{e,max,\ MLM2E}$	94.25	129.71	168.67	936.16	2553.95	6.67E8	58.07	621.99	2038.15	5.06E5
R^2	0.8850	0.9764	0.9940	0.9721	0.7116	0.9595	0.5351	0.9036	0.9917	0.9985
χ^2	131.86	46.37	22.47	653.24	173.61	265.28	196.37	7369.63	6504.14	1901.29
DLM2E										
n	1.74	0.64	0.64	0.36	0.55	0.32	0.59	0.36	23.33	0.75
D	27.11	126.60	192.02	620.33	28.26E4	1.10E6	49.63	1132.32	86.09	1.00E6
C_{01}	1.37E28	0.99	20.65	1.91E44	1.19E6	5.41E12	3.47E28	31.37	32.22	3.27E6
C_{02}	0.10	0.81	14.11	16.60	3730.10	5.90E7	0.02	16.55	1.61E16	3.96E4
$q_{e,max,\ DLM2E}$	94.34	162.05	245.79	446.64	3.11E5	7.04E5	58.56	815.27	4016.96	1.50E6
R^2	0.9617	0.9634	0.9212	0.9430	0.8325	0.8433	0.8450	0.7839	0.9461	0.9755
χ^2	43.95	71.78	297.04	1336.29	100.84	1026.20	65.46	1.65E4	4.21E4	3.05E4

V. Comparative studies

Table SI 5: Physicochemical characteristics of commercial ACs compared to AC850°C2h.

Activated carbon	Shape	Precursor	Activation method	A_{BET} (m^2/g)	V_{tot} (cm^3/g)	V_{mes} (%)	V_{mes} (cm^3/g)	V_{mic} (cm^3/g)
AC850°C2h	Grains 0.5-2 mm	Wood waste	Steam	1110	0.630	33.5	0.211	0.419
Brita AC	Grains 0.5-2 mm	Coconut shells	-	1025	0.422	9	0.038	0.384
Filtrasorb 300	Grains 0.5-2 mm	Bituminous coal	Steam	885	0.442	26	0.115	0.327

Table SI 6: Adsorption capacities of various activated carbon-based adsorbents in the literature for the pollutants studied here.

Pollutant	Adsorbent	Origin	Activation method	A_{BET} (m^2/g)	C_i (mg/L)	Dose (g AC/L)	Contact time (h)	$q_{e\ max}$ (mg/g)	Reference
ATZ	AC850°C2h	Wood	Physical/steam	1110	1-30	0.2	24	96.0	This study
	PCPAC	Araca fruit husks	Chemical/$FeCl_3$	431	5-40	1	3	21.7	[100]
DEA	AC850°C2h	Wood	Physical/steam	1110	0.5-30	0.2	24	129.1	This study
	ACF	Rayon	Physical/steam	1461	0-2	0.002	48	150.0	[99]
ESA MET	AC850°C2h	Wood	Physical/steam	1110	1-100	0.2	24	165.2	This study
	S-KC	Sunflower seed shells	Chemical/K_2CO_3	2024	5-150	0.1	3	218.0	[94]
	R-KC	Rape straw	Chemical/K_2CO_3	2220				273.0	
	AQ630	Jacobi-Commercial	Physical/steam	1016				93.0	
PARA	AC850°C2h	Wood	Physical/steam	1110	1-500	0.2	24	396.0	This study
	AAC	Artichoke leaves	Chemical/ $ZnCl_2$	1203	10-200	0.5	24	215.0	[41]
	PC	Pomegranate peels	Chemical/ $ZnCl_2$	1095				143.0	
CBZ	AC850°C2h	Wood	Physical/steam	1110	1-16	0.2	24	75.9	This study
	MACX3	Primary sludge	Chemical/KOH	795	0.6-16.5	0.025	4	134.0	[84]
	ACMW	Primary sludge	Chemical/KOH	1082				198.0	
CIP	AC850°C2h	Wood	Physical/steam	1110	1-100	0.2	24	253.3	This study
	GAC	Lignocellulosic	Chemical/H_3PO_4	940	13-83	1.1	24	221.0	[101]
17 BE	AC850°C2h	Wood	Physical/steam	1110	0.05-3	0.05	24	57.1	This study
	MAC	Macadamia nutshell	Unknown	-	1-10	0.1	2	22.0	[102]
PFOA	AC850°C2h	Wood	Physical/steam	1110	5-500	0.2	24	1977.3	This study
	BC-P(SB-co-AM)	Wood chips	Polymer(N)-doped biochar	167	2 - 100	0.1	24	536	[103]
PFOS	AC850°C2h	Wood	Physical/steam	1110	5-400	0.2	24	669.5	This study
	BC-P(SB-co-AM)	Wood chips	Polymer(N)-doped biochar	167	2 - 100	0.1	24	634	[103]
PFHxA	AC850°C2h	Wood	Physical/steam	1110	10-1000	0.2	24	3134.7	This study
	Bio-SBAC	Bio-solid sludge	Chemical/ $ZnCl_2$	723	0.05-0.75	1	24	0.7	[86]

VI. Analytical methods

Residual concentrations of PFOS, PFOA, PFHxA and MET ESA were determined by Ultra-Performance Liquid Chromatography coupled with quadrupole time-of-flight UPLC/MS/MS QTOF Xevo G2-XS Tof mass spectrometer. The solution containing the target compounds was injected into an ACQUITY UPLC HSS T3 column, with 110 Å pores and 1.8 µm particles.

The mobile phase consisted of two solvents: solvent A, ultrapure water with 0.1% formic acid, and solvent B, methanol. An initial combination of 60% solvent A and 40% solvent B was delivered at a flow rate of 0.4 mL/min. The percentage of solvent B in the mobile phase increased linearly over the first five minutes to reach a combination of 5% solvent A and 95% solvent B. This proportion was maintained until the ninth minute of analysis, when the initial combination was restored after ten minutes of analysis. Total run time was 13 minutes.

Column temperature was maintained at 40 °C. The determination coefficients (R^2) of the calibration curves for PFOS, PFOA, PFHxA and MET ESA were 0.9996, 0.9996, 0.9982 and 0.9973, respectively.

Residual concentrations of 17 BE were determined by Ultimate 3000 high-performance liquid chromatography (HPLC) using a Kinetex EVO C18 (150 × 2.1 mm, 10 µm) column. UV absorption wavelengths of 280 and 320 nm were used to quantify 17 BE. The mobile phases used were A (water + 0.05 % formic acid) and B (acetonitrile + 0.05 % formic acid) with a flow rate of 0.5 mL/min. The determination coefficients (R^2) of the 17 BE calibration curve was 0.9993.

Finally, the residual concentrations of ATZ, DEA, PARA, CBZ and CIP were measured using a UV-Vis spectrophotometer (Perkin-Elmer Lambda 35, USA) at wavelengths specific to each micropollutant, as shown in Table 1.

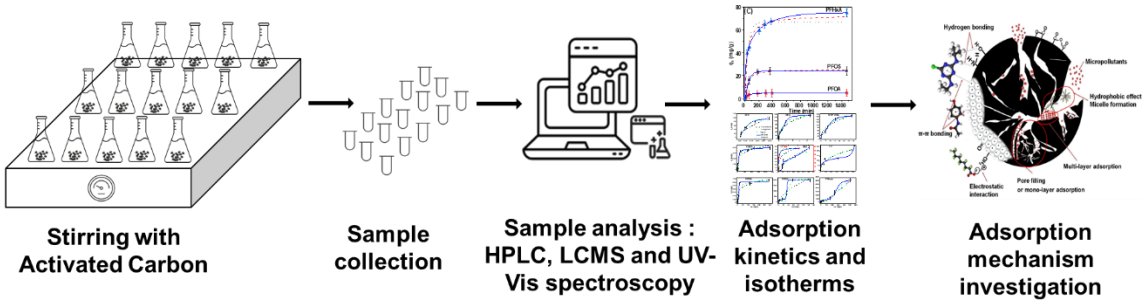

Figure SI 6: Diagram of experimental setup and successive steps.

VII. BSf (adsorption kinetics) and GBS (adsorption isotherms) models

The use of these models in this work is based on their ability to realistically capture the complex and heterogeneous characteristics of adsorption systems, overcoming the limitations of conventional models which are often based on simplifying assumptions. In our study, the fractal and stochastic models were chosen specifically for their relevance in describing the heterogeneity of surface-active sites as well as the diversity of adsorption mechanisms through the following elements:

- **Description of fractality and heterogeneity**: The fractal and stochastic models make it possible to quantify the fractality of the adsorbent surface, which results from the heterogeneity that can be chemical (different types and densities of surface functions) and morphological (different pore shapes: cracks, cavities, fissures, pitting and significant variations in pore size). This variability in pore shape and size is often ignored in simpler models, but is crucial for an accurate understanding of the adsorption process.
- **Estimation of non-integer reaction order and overall kinetics**: As well as quantifying fractality and heterogeneity, these models allow a non-integer reaction order to be extracted, reflecting more realistic adsorption kinetics adapted to the systems studied. The non-integer order provides a better representation of multi-scale diffusion processes and the complex interactions between adsorbed molecules and heterogeneous surface sites. In this

way, the use of these models facilitates a more detailed description of the overall adsorption kinetics.

- **Determination of the characteristic equilibrium time**: The BSf model provides an estimate of the characteristic time, i.e., the time required for the system to reach equilibrium or pseudo-equilibrium. In the case of systems where equilibrium is not completely reached, the BSf model can estimate it. This measurement is essential for assessing the speed of the process and its practical application particularly on an industrial scale.
- **Flexibility for inhomogeneous systems**: The GBS model is a generalization of the Langmuir and Freundlich isotherm, adapted for systems with inhomogeneous adsorption sites. This model is particularly advantageous when adsorption follows a continuous binding energy distribution, as is often the case for heterogeneous surfaces.
- **Ability to model complex isotherms**: Thanks to its versatility, the GBS model can be adapted to different forms of adsorption isotherms. This modelling capability makes it possible to explain complex behaviors that often occur with adsorbates of varying properties or in non-uniform surface environments.
- **Energy distribution and entropy**: The GBS model can be used to determine the adsorption energy distribution of molecules on the surface. This makes it possible to obtain information on the distribution of high and low energy sites, which helps to understand adsorption properties in both low and high solute concentration regions by applying the PDF probability density function. Entropy also can be determined using the GBS model by the application of Lagrange optimization method